Organisms
Journal of Biological Sciences

Vol. 2, 1 (JULY 2018)
ISSN: 2532-5876
DOI: 10.13133/2532-5876_3.14

ORIGINAL ARTICLE

Fractal values of metal micro-aggregates in lung microenvironment associated with tumor complexity

Rodolfo Guzzi[a] *and Rita Stefani* [b]

[a] *Systems Biology Group Lab, Dept. of Experimental medicine, Sapienza University, Rome, Italy*

[b] *Sant'Andrea Hospital, Rome, Italy*

Corresponding author: Rodolfo Guzzi rodolfoguzzi2@gmail.com

Abstract

Quantitative analysis, using scanning electron microscopy (SEM) and energy dispersive x-ray analysis (EDAX), of inorganic particulate found in lung tissue has been carried out for different lung pathologies. Results show a marked correlation between adenocarcinoma and carcinoma in presence of heavy metals. Such association was not found on specimens related to before the massive Italian industrialization of the 1960's. Most of the particles analyzed proved to be part of a coarse mode distribution. When their shapes were fibrous, they may be explained with fractal dimension. The aggregation processes have been simulated by a Diffusion-Limited Cluster Aggregation (DLCA) model. Results show that the significant part of the particulate matter was found in macrophages and has a fractal dimension that derives from a process of local aggregation of smaller particles rather than due to inhalation of larger coarse particles. Disruption of macrophage and tissue architecture due to aggregate deposition is significantly associated with lung cancer incidence.

Keywords: fractal analysis; inorganic particulate; cancer microenvironment

Citation: Guzzi, R, Stefani, R, 2018, "Fractal values of metal micro-aggregates in lung microenvironment associated with tumor complexity", *Organisms. Journal of Biological Sciences*, vol. 2, no. 1, pp. 73-81. DOI: 10.13133/2532-5876_3.14.

1. Introduction

Carcinogenesis of lung cancer is a complex and heterogeneous process. Improvements in our understanding of alterations at multiple levels (microenvironment, genetic, epigenetic, protein expression) and their functional significance have the potential to impact on lung cancer diagnosis, prognosis, and treatment. Lung cancers develop through a multistep process involving the microenvironment, the development of multiple genetic and epigenetic alterations, activation of growth-promoting pathways and inhibition of tumor suppressor pathways. Recently, studies on tumor have shown that microenvironmental factors promote oncogenesis at the tissue level (Bissel, Hatle, and Calvin, 1979, Barcellos-Hoff 2010). Numerous authors have demonstrated the tumor microenvironment not only responds to and supports carcinogenesis, but actively contributes to tumor initiation, progression, and metastasis. These issues have been addressed by the Tissue Organization Field Theory (TOFT) (Soto and Sonnenschein, 2011; Bizzarri & Cucina, 2016), which focus on cancer as 'development gone awry', due to disrupted properties of the surrounding milieu. TOFT argues that the focus of the Somatic Cell Theory (SMT) (Bedessem & Ruphy, 2015) on single cell events is inappropriate and misses a whole range of effects at the level of tissue organization, ultimately resulting in creating a pathological environment in which those mutations can accumulate. Aberrant disruption of the field can therefore produce aberrant structures without requiring any genetic changes (Bizzarri & Cucina, 2014).

Herein, we aim to investigate how aerosol particulate may disrupt the architecture of lung microenvironment, including stroma and macrophages, and how such changes are associated with lung cancer incidence.

The structure of the respiratory tract is such that larger particulates are filtered out, or deposited in the more proximal portions. Only smaller respirable particles penetrate deeply into the lung. The aerodynamic behavior of the particles is determined, not only by their size, but also by their shape and density. This behavior is expressed in terms of a mass median aerodynamic diameter, which equates the particle behavior to that of a sphere of unit density. The shapes are defined as fibrous when the particles have an irregular shape, or compact when approximating a sphere or a regular solid. There are four deposition mechanisms: sedimentation, inertial impaction, interception and diffusion. Sedimentation is responsible for the deposition in large airways of particles with an aerodynamic diameter of around 2 microns. It is influenced less by the length and shape of the particles than the falling speed of the particles which is determined by gravity, their density and cross-section area. Inertial impaction is responsible for most of the deposition in the nose and larger airways involving particles larger than 10 microns in diameter. As for sedimentation, the density, diameter and cross-section of the particle as well as change of direction and rate of airflow in the airway influence impaction. Interception is responsible for deposition of irregular and fibrous particles. Long fibrous particles tend to orient with the air stream and avoid sedimentation and impaction until they are intercepted by collision with the walls of the terminal respiratory bronchioles. Diffusion only affects the very small particles (around 0.1-micron diameter). It influences the deposition of the smallest particles which is independent of their density. As most of calculations are based on theoretical models, the previous statements may be considered as relative rather than absolute. In fact, the pattern of respiration can significantly influence particle deposition. With a higher tidal volume, there is a deeper penetration of air in the lungs and with increasing breathing rates the time for particles to become deposited decreases. During massive physical effort the product of the tidal volume and number of breaths per minute increases and thus there is greater particle deposition than at rest. Atmospheric aerosols may be classified concerning size distribution models. Mass size distributions of urban aerosols correspond to log-normal distribution with different modes. The current classification defines an accumulation mode (AM) the size distribution with aerodynamic diameters ranging from 0.1 to 1micron, as coarse mode (CM) the size distribution for particles above 1 micron, and nucleus mode (NM) for particles with sizes of less than 0.1 microns.

We used an SEM-EDAX, to analyze the chemical and physical properties of inhaled particles. This approach enabled us to develop a method of analysis based on studies of the fractal dimension of the aerosol and the mechanisms of their accretion. We further established a correlation between the physical-chemical structure of aerosols aggregate absorbed by macrophages, and occurrence of lung cancer vs a sample of healthy controls, patients with non-cancerous lung diseases.

2. Material and methods

2.1. Patients and histological samples

Our study was performed on 1000 measurements related to 87 patients, as previously described (Guzzi *et al*. 1996). Bioptic and autoptic lung specimens were collected from patients with no lung diseases (the control group) and patients with fibrosis, silicosis, carcinoma, adenocarcinoma (the experimental group). Bioptic sampling methodology was the same for all specimens. Analysis was carried out by focusing on the shape of the particle(s), and on their chemical composition. All patients lived in the Po Valley (Italy). To gain information about the incidence of particles deposition during a less intensely industrialized period, we extended our analysis to biopsies performed before 1960 (in Italy the 60's can be considered the years of the introduction of the massive industrialization) in patients from the same geographic area. Overall, 69 subjects were enrolled along this second survey.

2.2. Electron microscopy

The resolving power of the Scanning Electron Microscopy (SEM) combined with Energy Dispersive X-ray Analysis (EDXA or EDAX), introduced by De Nee et *al*. (1974) and by Abraham (1974, 1978) and Amorico *et al*. (1989) allow us to examine the physical-chemical features of the particulate matter collected both in the natural environment and in lung macrophages. SEM-EDAX measurements were carried out in areas where optical microscopy observed an apparent particulate concentration. The particles detected were analyzed regarding their location and size, shape and

elemental composition. Paraffinized tissue samples, obtained by lung biopsy, were cut in thin slices, by a microtome, and deparaffinized. One should recall that approximately 90% of the tissue weight is water, which is removed during dehydration, before placing the specimen in the SEM vacuum chamber. The thin slices of tissue were glued with conductive carbon and coated with clean carbon. An accurate patient's anamnesis was carried out to avoid any correlation between tobacco exposure risk and potentially related pathology. Therefore, smoking patients were excluded from our present investigation.

An example of SEM EDAX results is shown in Figure 1 in which are reports both the image of the particle, its size, elemental composition and the associated disease.

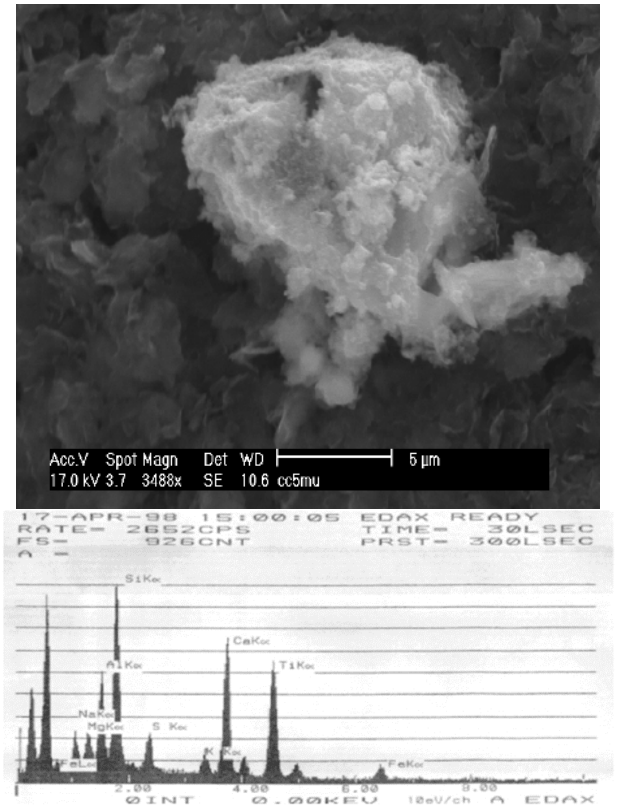

Fig. 1. Example of SEM-EDAX analysis carried out on fibrous particles (Upper figure). Pathology: Carcinoma Elemental composition Fe, Al, Ti, S, P,O, Mg, Na, Si, K (Lower figure).

We selected the macrophage content to show the type of particulate matter inhaled and subjected to sedimentation in the lung. We ignored particles subjected to diffusion (consequently, as already cited, smokers were excluded from our analysis), and those subject to inertial impaction. Our samples concern phagocytic macrophages, which are correlated with phagocytosis phenomena. These are active *in vivo* phenomena and consequently any external contamination can be excluded. The use of biopsy preserved in paraffin, avoiding the process of decomposition, permits one to compare samples collected at different times. In cases where tumors were identified, particles found in neoplastic and in adjacent, non-cancerous tissues were analyzed.

2.3. Mathematical modelling and fractal analysis

The simplest method to analyze findings from the SEM EDAX images is to use the Box-Counting Method, even though it is recognized to have a lot of shortcomings (Iannaccone & Khokha, 1996). We start from extracting the boundary, which is the fractal object. Counting boxes with at least one white pixel can be calculated more efficiently using Integral Image, a technique introduced by Viola-Jones (2004). Then, the mass (white content) of a region is obtained from the area delimited by two corner points. Therefore, instead of partitioning the image, one can get a list of all the boxes of a given size. Kamer et al. (2013) suggest an improvement of the box-counting method. Renyi (1970) claims that, first of all, it is important to point out that if we are only checking if a box is empty or not we are effectively measuring the D_0, the box-counting dimension. By referring to D_0 as the fractal dimension, we are assuming that our object is a mono-fractal, i.e., that all its generalized dimensions Dq are equal, where

$$D_q = \lim_{\varepsilon \to \infty} \frac{\frac{1}{1-q} \log \sum_i^N p_i^q}{\log \frac{1}{\varepsilon}}$$

with D0=D1(entropy dimension)=D2(correlation dimension) and so on… and where ε is the scale of observation, pi(ε) is the fraction of data points (e.g., estimated measure) within box i of size ε ; q is a real-valued moment order, and the sum is performed over all boxes covering the data set under investigation

However, even if you assume that the object is mono-fractal, review literature of fractal dimension estimation concludes that the box-counting method is a poor choice (Theiler, 1990). The fundamental principle in fractal dimension estimation is to study the object at different scales (Kamer *et al.* 2013). The question is how to sample this continuum of scales. There are two different class of methods. The first one is the fixed-sized method that counts the number of points in a fixed size region (boxes/spheres). It performs poorly because one never knows how boxes grow. The second is the fixed-mass method that improves the box by reaching over to

their *n*th nearest neighbor. In such a way, one always assures that it is covering the same mass.

Even though the fixed-mass method is more robust than fixed-size methods, both suffer from finite-size and edge effect. Then one needs some extra measures to avoid the edges of our object; otherwise at larger scales (of mass/size), one starts to get off this leveling effect.

Biennia	Lung n. of cases Cancer#	SC	ADC	SCC	LCC
1963-1964	42	19	2	3	18
1973-1974	293	143	26	67	57
1983-1984	637	358	127	96	56
1993-1994	738	406	225	90	17

Table 1. Distribution of histological type from 1963 to 1994. SC=Squamous Carcinoma; ADC= AD, Adeno Carcinoma; SCC=Small Cell Carcinoma; LCC= Large Cell Carcinoma (adapted from Guzzi et al 1996).

The method by Kamer et *al.* 2013. incorporates two motivated criteria (barycentric pivot point selection, and non-overlapping coverage) to reduce edge effects, improve precision and reduce computation time. Implementation of the method on synthetic benchmarks demonstrates the superior performance of their method compared with existing alternatives routinely used in the literature. They also use the technique to estimate the multifractal properties of the widely studied growth process of Diffusion Limited Aggregation. We have adopted their method to define the multifractality of our particles. In order to understand more about the "fractality" of the particles we also created stereoscopic images using the MeX software (by Alicona) which produces the 3D view of stereoscopic SEM images. Measurements were performed by positioning the viewed specimen in a way that it is in a position to determine the final DEM (Digital Elevation Model). Since typical stereoscopic values range from 1 to 7 degrees, we put our viewer specimen around 4 degrees to create the correct tilting angle to produce the stereoscopic images. Figure 2 contains the 3D image sample as provided by this approach. This figure has been used to define the complexity of the particle.

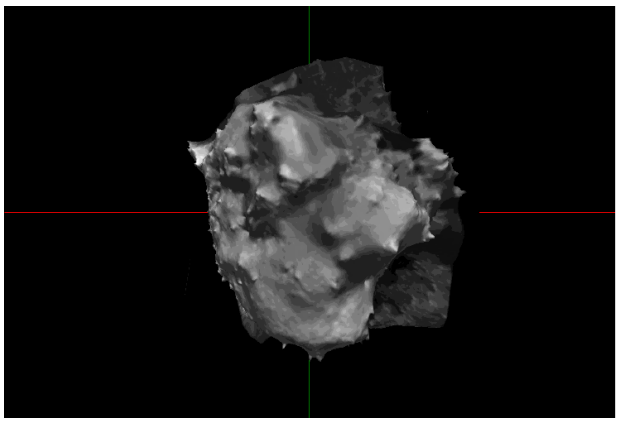

Fig. 2. Stereoscopic image of the particle of Figure 1, obtained by SEM image.

3. Results

3.1. The relationship between pathology findings and elemental composition of the particles present in macrophages

Distribution of lung cancers and non-malignant diseases among the different groups and periods is reported in Table I. The comparison between our findings obtained on pre-1960 and post-1960 shows that after the 60's Squamous Carcinomas (SC) and Adeno-Carcinomas (ADC) both increase exponentially. Our specimens were divided into three main groups related to the locality in which the patients lived: urban, rural and higher altitude sites. This selection was chosen by a long-term air sampling carried out in urban and hill locations. We did not consider the rural areas because they are currently comparable to the urban conditions, at least in the Po Valley. The results of such sampling are presented in Table II for urban and hill areas.

The sets of case studies are reported in Table 3. Specimens taken from patients resident in urban sites show the higher concentration of particulate matter with a marked presence of Cu, Ag, and Zn. Vanadium (V) was present in only one case of adenocarcinoma. To find a possible relationship between elements and diseases, we reconsidered our findings according to the ANOVA test. Results are shown in Table IV. The test of significance shown in Table 4 indicates a significant correlation (indicated by *) between lung disease and the percentage of the different elements found.

Ag is associated with Squamous Carcinoma, while Cu, Ni, and V are associated with Adenocarcinoma. Comparing Table IV with Table II, we see how distribution of aggregated elements values found in lung

macrophages mirrors the distribution of the same elements recorded during field measurements in urban and hill sites. Ag and Cu were not found in this investigation.

Element	Mean	σ	Mean	σ
Ag	-	-	-	-
Ni	0.27	0.44	4.16	2.09
Cu	-	-	-	-
Ti	0.12	0.28	-	-
Na	2.48	4.58	2.85	2.36
K	5.78	11.81	0.59	0.82
Mg	3.35	6.28	4.90	2.97
Fe	3.09	3.43	27.88	17.47
Ca	24.92	25.31	0.23	0.54
Zn	0.59	1.45	-	-
Cr	0.50	0.66	10.53	6.19
Al	8.59	11.07	13.30	5.44
V	0.75	-	-	-
Cl	5.72	14.68	0.47	0.44
P	7.97	10.68	4.31	3.82
S	13.21	11.68	19.82	18.08
Si	19.14	16.18	10.95	4.60

Table 2. Elemental composition (in percent) of airborne particulate matter (coarse mode distribution) collected in urban and hilly sites (adapted from Guzzi et al 1996). The second and third columns refer to urban measurements, while the fourth and fifth columns are for hill measurements.

The elements found are listed in the first column of Table II. It means that there is a direct link between atmospheric aerosols collected in the natural environment and those inhaled.

The nine specimens taken before the 60's contain no more than ten elements. Ag, Ni, Cu, Ti, Zn, Cr, and V are absent. From the correlations between some of these elements and recent pathologies like such as Squamous Carcinoma and Adenocarcinoma as shown in Table IV, one may argue that the absence of such pathologies before the 60s, might be due to the lack of aerosols containing such elements.

3.2. Extraction and modeling the particles by aggregation

Recently pattern-formation processes have been of scientific interest because it has been shown that even straightforward non-linear systems can lead to complex, often chaotic behavior which can be described by fractal geometry. Random dendritic growth (Ball, 1986) seems to be close to the processes observed here. Forest and Witten (1979) used the fractal concept (Mandelbrot 1977) to describe aggregates of metals. Fractal aggregates are scale invariant, and this concept includes a mathematical description and the quantifiable Haussdorff parameter or fractal dimension D (Hausdorff, 1919).

Case studies	# of occurrence
Normal (pre-1960)	9
Normal (post-1960)	11
Fibrosis	10
Adenocarcinoma	19
Carcinoma	27
Silicosis	1
Benign tumour	4
Peumothorax	6

Table 3. Case studies (adapted from Guzzi et al 1996).

The scaling behavior does not apply to all length scale in a real system.

The fractal in Figure 1 is characterized by an upper cut-off length (R) which equals the radius of the cluster and a lower cut-off length (a), equal to the radius of the primary particles. The fractal dimensionality (D) does apply to length scales between *a* and R. The concept of fractal aggregates may be described by the following expression:

$$N = K_0 (R_g/a)^D \qquad (1)$$

Where N is the number of primary monomers proportional to the mass in the aggregate, $R = R_g$ is the radius of gyration or a measure of the overall aggregate radius, K_0 is a proportionality constant usually of order unit, D is the fractal dimension. It is straightforward to find D by a least-squares fit applied to a log-log transformation on equation 1. In colloids and aerosols, clusters meet other clusters through a random process and this process can be described by diffusion-limited cluster aggregation (DLCA) because the role-limiting step is the diffusive motion of the clusters (Meakin 1983, 1988; Kolb *et al.* 1983).

In this situation, D is on the order of 1.75 – 1.8. In case of motion between collision to be a straight line (ballistic) rather than a random walk and then D is of the order of 1.9 (Meakin, 1984). In colloids, solute modification of the double layer surrounding the particles can drastically reduce the sticking probability and then the reaction limited cluster aggregation (RLCA) where D is in order of 2.1 to 2.2 (Weitz et *al*. 1985). As mentioned before most of the particles were related to coarse mode. In general, this particulate matter should be subject to sedimentation in the larger airways. Furthermore, apart from a few spherical particles of Fe (see Figure 3) and well-defined particles of Al (see Figure 4), particulate matter found in the lungs seemed to derive from accretion processes.

Element	Site	Site	Histology	NNV	NV	Sex
	Urban	Hill				
Ag	*		SC		*	
Ni	*		ADC		*	
Cu	*		ADC,SC,PT	*PT	*ADC,SC	
Ti						
Na	*		B,F,PT	*PT		
K						
Mg						
Fe			B			
Ca			N,B			
Zn			SC,B		*	
Cr						
Al			PT	*		
V	*		ADC		*	
Cl	*		N,B,PT	*PT	*N,B	*
P			N,B			
S			ADC,B	*	*	
Si	*	*	ADC,SC,S	*S		

Table 4. Test of significance: NNV=Non Neoplastic Volume; NV=Neoplastic Volume; SC=Squamous Carcinoma; ADC=ADeno Carcinoma; B=Benign Tumour; N=Normal; F=Fibrosis; S=Silicosis; PT=PneumoThorax. The more significant correlation between element presence and pathology is indicated in the columns NNV and NV with an asterisk. An asterisk without any prevailing pathology means that all the pathologies in the histology column are significant (adapted from Guzzi et al. 1996).

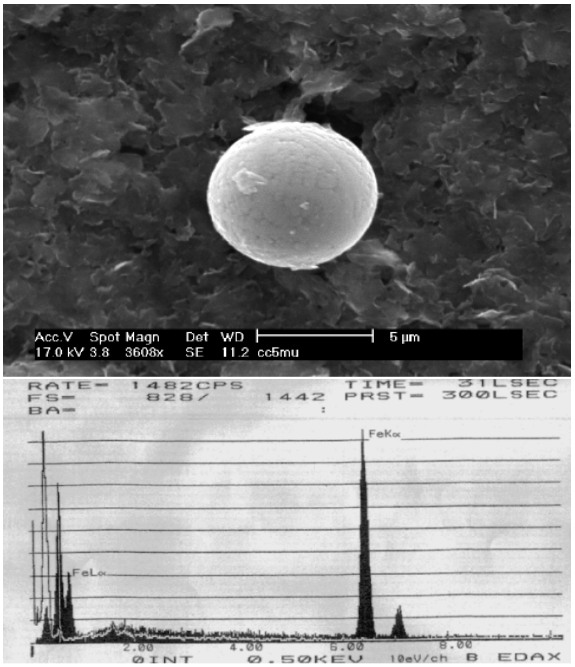

Fig. 3. Spherical particle Upper figure) of Fe as identified by EDAX, in the lower figure.

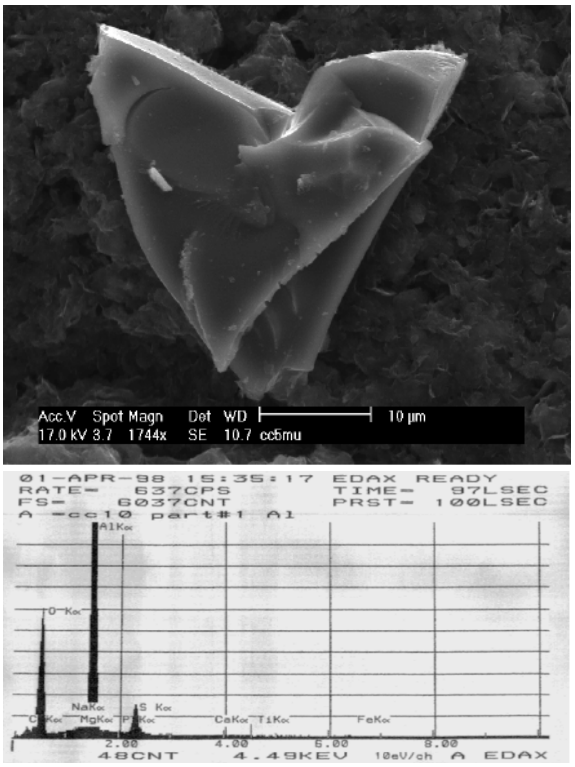

Fig. 4. Non-Spherical particle (Upper figure) of Al, identified by EDAX in the lower figure.

Accretion is a process in which particles move around until they encounter and adhere to another particle, irregularly shaped clusters being formed. Fibrous particles suggest the presence of an endogenous aggregation mechanism. The particles inhaled, having a size of around 0.1 microns, reach the lung where they

aggregate to form larger particles such as those analyzed here (Kolb et *al*. 1983). To better understand the growth mechanisms of particles we have used a Diffusion-Limited-Cluster-Aggregation (DLCA) model used previously in biological processes. The sticking processes were taken into account by introducing a factor of correction of this effect. In the DLCA model, particles are added, one at a time, to a growing cluster via random-walk trajectories, originating outside of the region occupied by the cluster. This process leads to the formation of a random fractal structure with a fractal dimensionality substantially smaller than that of the space in which the aggregate is embedded. A simple three-dimensional DLCA model can be developed with a gyration radius (R_g) measured from the original seeding of growth site that can be considered the actual size of the aggregate. The particle is placed on a randomly selected site at a distance $R_s > R_g$. If the particle follows a trajectory that eventually brings it to an empty perimeter site, it remains, and the cluster grows. Alternatively, particles may follow a path that finally takes it away from the cluster (for instance a distance R_s with $R_s = 3R_g$) where the trajectory is terminated. In such a case, the particle is annihilated, and a new random walk trajectory is started from a randomly selected site on the launching circle. This procedure is repeated many times until a large cluster has been generated. From what has been said so far it is apparent that an effective fractal dimensionality exists and the fractal dimension is the way of characterizing scale changes between the object and its self-similar parts.

3.3. Fractal measures and DLCA method

The procedures above described has been applied to our samples. As an example, an analysis was carried out in the area shown in the Figure 5 where we explained the correspondent fractal dimension.

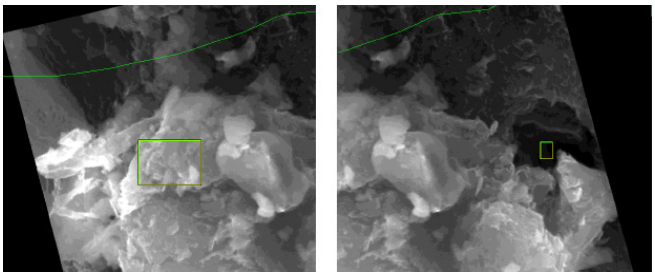

Fig. 5. Example of fractal analysis of a particle. D= 1.57 (left). Sampling has been carried out on selected area. All the sample has been analyzed at different regions giving similar values. Sampling area in which the particle is not present gives D≈ 2.001 (right).

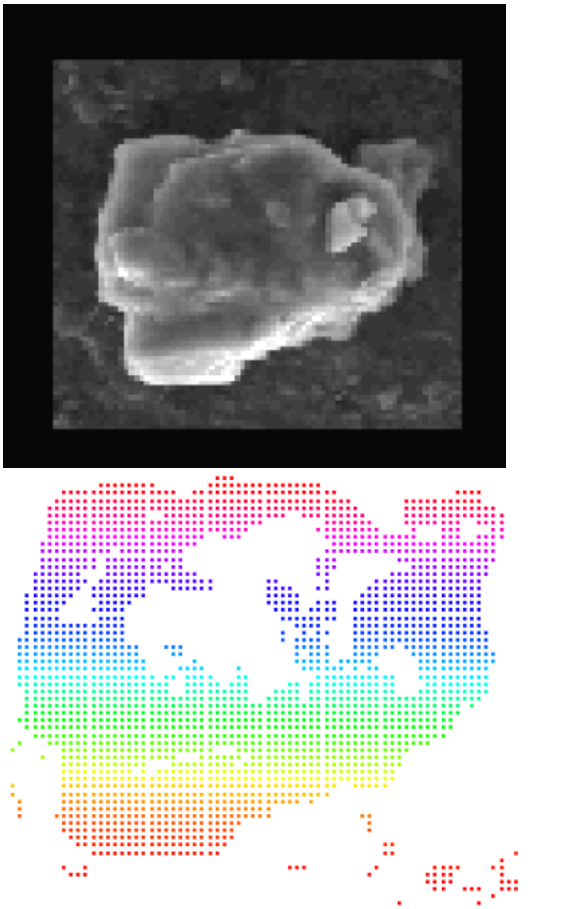

Fig. 6. Comparison between an aerosol sample (Upper, SEM image) and that has been reconstructed via DLCA simulation (Lower image). In Table V we show the fractal dimension of some selected particles and that obtained by DLA model.

Up to the fractal value D≈ 1.8 we have the case of Diffusion Limited cluster-cluster aggregation (DLCA), for D≈ 2.1 we have the Reaction limited cluster-cluster aggregation (RLCA) regime typical of colloids where solute modification surrounding the particles can drastically reduce the sticking probability (Weitz *et al*. 1985, Lin *et al.* 1990) as appear to be in the phagocytosis process. If we use the fractal values formed from our samples to reconstruct the particle shape using the DLCA model we can obtain similar configuration as shown in Figure 6 shows that irregular particles are due to a process of local accretion.

From the Table V, we see a good agreement between the fractal dimension obtained for different SEM image and those derived from DLA model. We have also introduced the value of the seed in such a way as to add in the random process precisely those values obtained from the measurements made on the fractal aggregation. In case of Erionitis the samples have a fractal dimension higher than two (FD >2), and thus cannot be simulated by DLA. In the last column, we show how the sample can be redrawn by DLA model.

Specimen (n)= number analyzed samples	Fractal Dimension of the object	p	Fractal Dimension	DLA Radius-No Particles-Seed
CC(7)-Simple	1.17+-0.1	0.44	1.17+-0.08	4/80/1
ADC(4)-Simple	1.25+-0.2	0.75	1.25+-0.06	2/150/5
CC(9) Complex	1.29+-0.1	1	1.3+-0.1	4/70/5
ADC(5)-Complex	1.55+-0.1	1	1.55+-0.09	2/90/9
PN(11)-Simple	1.18+-0.2		1.18+-0.05	4/10/5
PN(9-)Complex	1.37+-0.1		1.37+-0.09	3/90/7
E(5)-Simple	2.05+-0.1	1	-	-
E(7)-Complex	2.08+-0.1	1	-	-

Table 5. Comparison between the fractal dimension calculated by the SEM image and the image obtained by the simulation with DLA. CC=Carcinoma; ADC=Adeno Carcinoma; PN=Pneumothorax; E=Erionitis. The number refers to the sample analyzed. Simple means the particulate matter is compact, while complex means the particulate matter is spread into the macrophage. The number into the brackets, next to the disease, indicates the number of samples analyzed.

We have used a visual comparison that fails when there is no overlapping between the DLA simulated image and SEM image. Even though the technique of modeling the particle aggregation need to be improved, our exercises show existing some peculiarities between the modality of aggregation and its fractal dimension that can be used to learn more about the accretion processes in lungs.

4. Discussion

Quantitative information on particulate tissue burden in the lung is essential for investigating relationships of particulates to several aspects of the disease, such as exposure, physiology, and pathology. Quantitative analysis using SEM and EDAX of inorganic materials found in lung tissue show that are reproducible results for different pathologies. This approach gives the size and shape of particulate matter present in macrophages and relative element composition. Statistical analysis carried out on 87 patients shows that fractal dimension (FD) increases roughly linearly in cancerous specimens, from the simplest to the more complex architecture of the examined tissue specimens (from carcinoma to complex adenocarcinoma). At a first glance, higher FD are associated with wider disruptive effects on the microenvironment and, consequently, with higher cancer risk. Indeed, in a previously epidemiological study carried out on tissue specimens obtained before 1960 (i.e., before the onset of massive industrialization), we showed a total absence of heavy metals and no presence of adenocarcinoma and carcinoma (Amorico et *al*. 1989). In the present investigation, since most of the particles had sizes of about 2 - 5 microns and because their shape was irregular, we argue that they are due to aggregation of smaller particles regular apart homogeneous particles as those of Fe and Al. The p-value, obtained by the Z-test vs test group and pneumothorax (see Table V), indicating for ADC a value of 1 supports the null hypothesis that the samples are comparable to a simple random sample from the population of reference (PN). The presence of Erionitis can produce mesothelioma, but in this case the patient was affected of benign asbestos - related pleural effusion and not of malignant pleural mesothelioma. Furthermore, analysis of fractal dimension of particles shows that they are linked to a value that is typical of RLCA regime. Results obtained from the DLCA model indicate that there is a strong correlation between the fractal dimension obtained by the DLCA model and that one got from SEM image showing that coarse particles are derived from local aggregation mechanisms rather than from the inhalation of larger particles. The current SEM technique has been also improved to take the stereoscopic view to take into account the tri-dimensional structure of the particles. The present experiment does show that there are some peculiarities between the modality of aggregation and its fractal dimension which could be used to learn more about the accretion processes of particles and their incidence in lung diseases. Overall, these findings suggest that specific dynamics of the microenvironment are crucial in determining the shape acquired by mineral aggregates and consequently in constraining their effects on lung tissue (Min Hu &

Polyak, 2008). This experiment opens a door in favor to TOFT paradigm since the aggregation modality seems due to the previous inflammatory process of lung stroma. However, we believe we should develop a multiparameter assessment of immune and inflammatory cell composition of human lung cancer stroma in order to understand the relation between the fractal structure of aerosol in macrophages and the fractal structure of tumor, which is beyond the scope of the present study.

Acknowledgments

We thank Prof. Giuseppe Barbolini for biopsies supplied, Dr. Giorgio Gasparotto and Dr. Marco Chiarini for technical support.

References

Abraham, J.L. 1974 Documentation of environmental particulate exposure in humans using SEM-EDAX. *Scanning Electron Microscopy Part II SEM inc AMF O'Hare Illinois* vol 60616, pp. 259-266.

Abraham, J.L. 1978 *Recent Advances in Pneumoconiosis: the Pathologist's role in Etiologic Diagnosis. The Lung*. IAP Monograph No 19, The Williams & Wilkins. Baltimora Md The Inter. Acad. Pathol pp. 96-137

Amorico, A.M., Barbolini, G., Bisetti, A., Guzzi, R., Lazzaretti, G., Migaldi, M., Pellegrino, M. and Piscitelli, M. 1989 Identificazione e caratterizzazione del particolato solido endomacrofagico polmonare quale indice del pneumoclima in soggetti sani e affetti da varie pneumopatie. 1. Approccio metodologico e studio preliminare. *La Rivista della Tubercolosi* vol XXI, pp. 13-24.

Ball, R. C. 1986 *On the growth and form: form and non fractal patterns in physics*. Ed H. E. Stanley & N. Ostroswsky, NATO ASI Series E100.

Barcellos-Hoff, 2010 Stromal mediation of radiation carcinogenesis *Journal of Mammary Gland Biology and Neoplasia*, vol.15, no. 4, pp. 381–387.

Bedessem B, Ruphy S. 2015 SMT or TOFT? How the two main theories of carcinogenesis are made (artificially) incompatible. *Acta Biotheor*, vol 63, n. 3, pp. 257-67.

Bissell, M. J. Hatie, C, and Calvin M. 1979 Is the product of the src gene a promoter? *Proceedings of the National Academy of Sciences of the United States of America*, vol. 76, no. 1, pp. 348–352.

Bizzarri M., Cucina A. 2014 Tumor and the Microenvironment: A Chance to Reframe the Paradigm of Carcinogenesis? *BioMed Research International* 2014:934038.

Bizzarri M, Cucina A. 2016 SMT and TOFT: Why and How They are Opposite and Incompatible Paradigms *Acta Biotheor* vol 64, n. 3, pp. 221-39.

De Nee, P. B., Abraham, J. L. and Willard P A. 1974 Histochemical stains for the scanning electron microscopy. Qualitative and semiqualitative aspects of specific silver stains. Scanning Electron Microscopy. Part I. *Proceedings of 7th Annual Scanning Elect. Microscope Simposium IIT*, Research Institute Chicago Illinois vol 60616, pp. 259-266

Forest, S.R. and Witten Jr., T.A. 1979 Long-range correlations in smoke-particle aggregates. *J. Phys* vol A12, pp., L109-L117

Kamer, Y., Ouillon, G., & Sornette, D. 2013 Barycentric fixed-mass method for multifractal analysis. *Physical Review E*, vol 88, n 2, 022922.

Guzzi, R , Barbolini, G. and Migaldi. M. 1996 Contribution to the definition of an air quality index by biological sampling of lung macrophages: correlation with lung disease. *Physica Medica*, vol 12, n. 4, pp. 271-279.

Hausdorff, F. 1919 Dimension und aübers mass. *Math. Ann* vol 79, pp. 157-179.

Kolb, M., Botet, R. and Jullien, R. 1983 Scaling of kinetically growing clusters. *Phys. Rev. Lett* vol 51, pp. 1123-1126

Iannaccone, P.M, Khokha, M.K. 1996. *Fractal Geometry in Biological Systems*. CRC Press.

Lin, M.Y., Lindsay, H.M., Weitz, D.A., Ball, R.C., Klein, R. and Meakin, P. 1990 Universal reaction-limited colloid aggregation. *Phys. Rev* vol A41, pp. 2005-2020.

Mandelbrot, BB. 1977 *Fractals: form, chance and dimension* W. H. Freeman, San Francisco, CA.

Meakin, P. 1983 Formation of fractal clusters and network by irreversible diffusion-limited aggregation. *Phys. Rev. Lett*. vol 51, pp. 1119-1122.

Meakin, P. 1984 Effects of clusters trajectories on cluster-cluster aggregation: a comparison on linear and brownian trajectories in two and three-dimensional simulations. *Phys. Rev*. vol A29, pp. 997-999.

Meakin, P. 1988 Fractal aggregates. *Adv. Coll. Interface Sci.* vol 28, pp. 249-331.

Min-Hu, K. Polyak. 2008 Microenvironmental regulation of cancer development" *Current Opinion in Genetics & Development* vol 18, n. 1, pp. 27-34.

Renyi, A. 1970. *Probability Theory*. Amsterdam, North Holland

Soto AM, and Sonnenschein C. 2011 The tissue organization field theory of cancer: a testable replacement for the somatic mutation theory *BioEssays*, vol. 33, no. 5, pp. 332–340.

Viola P., M. Jones 2004 Robust real time object detection. *International Computer Vision* vol 57, n. 2, pp 137–154.

Theiler, J. 1990. Estimating fractal dimension. *Journal of the Optical Society of America A*, vol 7, n. 6, pp. 1055-1076.

Weitz, D.A., Huang, J.S., Lin, M.Y. and Sung, J. 1985 Limits of fractal dimension for irreversible kinetic aggregation of gold colloids. *Phys. Rev. Lett* vol 54, pp. 1416-1419.